



CHORUS

This is the accepted manuscript made available via CHORUS. The article has been published as:

Magnetoelastic parametric instabilities of localized spin waves induced by traveling elastic waves

Ivan Lisenkov, Albrecht Jander, and Pallavi Dhagat

Phys. Rev. B **99**, 184433 — Published 24 May 2019

DOI: [10.1103/PhysRevB.99.184433](https://doi.org/10.1103/PhysRevB.99.184433)

Magneto-elastic parametric instabilities of localized spin-waves induced by traveling elastic waves

Ivan Lisenkov,^{1,*} Albrecht Jander,¹ and Pallavi Dhagat¹

¹*School of Electrical Engineering and Computer Science, Oregon State University, OR, USA*

A theory of parametric interaction between spin-waves localized in a waveguide and traveling elastic waves is developed for ferromagnetic thin films. The presented theoretical formalism takes into account an arbitrary spatial distribution of the displacement field in the acoustic waves and an arbitrary magnetization in spin-waves. Using the theory, we examine interaction of forward-volume spin-waves (FVSW) localized in a narrow waveguide and Rayleigh surface acoustic waves traveling in a substrate underneath the waveguide. We show that, in contrast to classical electromagnetic pumping, the symmetry of the magneto-elastic interaction allows for the generation of first order parametric instabilities in spin-waves with circular precession, such as FVSW. At the same time the localization of spin waves modifies the momentum conservation law for the parametric process to include the transfer of momentum to the waveguide, which allows for a frequency separation of the interacting counter-propagating spin-waves. The frequency separation enables amplification of a localized spin-wave without generation of a counter-propagating idler wave, which results in a greater amplification efficiency.

I. INTRODUCTION

Parametric interaction of waves has been studied in a broad range of physical systems, e.g. in non-linear optics¹, plasma physics², acoustics³ and magnetism⁴ (for a review see Ref. [5]). The first order parametric interaction (or three wave processes) in bulk media manifests itself in the energy and momentum conservation laws⁵. The conservation laws define selection rules constraining which waves can parametrically interact. By Noether's theorem, the conservation of momentum derives from space translational symmetry. If the translational symmetry is broken, i.e. if the area of the parametric interaction is limited in space⁶, the global momentum conservation law allows transfer of momentum from the interacting waves to the confining structure, analogous to the radiation pressure effect⁷. As a consequence of the symmetry breaking, the selection rules for parametrically interacting waves are relaxed. For example, a localized electromagnetic pump allows parametric interaction of co-propagating spin-waves, while such interaction is not possible in the case of uniform pumping⁶.

The translational symmetry is broken when the interacting waves are localized in potential wells or waveguides. The fact that the waves can propagate only in the directions allowed by the waveguides is reflected in the momentum conservation law for these waves. Since these momentum conservation conditions are different from the bulk case, the wave localization opens an additional degree of freedom for fine tuning of the parametric interaction. As an example of such a system, in this work we study the parametric interaction of spin-waves, localized in a waveguide made of a magnetostrictive ferromagnet, with traveling *elastic* waves^{8–11}.

The parametric pumping of spin waves in thin ferromagnetic films by electromagnetic fields has been well studied^{4,6,12–17} and shown to be useful for sustaining and amplifying spin wave amplitudes. The non-linear pro-

cesses of magnetic parametric pumping have also been shown to find applications in analog signal processing¹⁷.

The electromagnetic parametric pumping process is based on the Zeeman interaction between the oscillating magnetic field (typically in the microwave frequency range) and the time-varying component of magnetization parallel to the equilibrium magnetization. This is conventionally termed “parallel pumping” since the pumping magnetic field is parallel to the magnetization. In this geometry, the coupling between the spin waves modes and the pumping field depends on the precession ellipticity¹² and vanishes for the spin waves having a circular precession. Therefore the parallel pumping works well for backward volume spin waves (BVSW) in thin films, where the wavevector is parallel to the in-plane equilibrium magnetization and the thin-film shape anisotropy results in elliptical precession. However, the dispersion of BVSWs is not a single-valued function of the frequency¹², leading to instabilities for short and slow dipolar-exchange spin waves⁶. These dipolar-exchange spin-waves are usually not usable in signal processing¹⁶, because their wavelengths are too short to pick up with conventional spin-wave antennas. Forward volume spin waves (FVSWs) propagate when the film is magnetized perpendicularly to its plane. FVSWs have a single-valued dispersion function¹², but since the magnetization precession is circular in the long-wavelength limit, they cannot be pumped electromagnetically.

The mechanism of acoustic parametric pumping is different. The energy of spin wave excitations depends on the magnetic anisotropy. Thus, in general, by modulating the magnetic anisotropy one can parametrically interact with spin waves. In magnetostrictive materials, the magnetic anisotropy can be modulated via the magneto-elastic interaction by deformation of the sample. The energy of the magneto-elastic interaction is quadratic in the magnetization (see (8) below), in contrast with the energy of Zeeman interaction, which is linear with the magnetization. The form of the magneto-elastic energy allows,

in particular, pumping of spin waves modes having a circular precession. The parametric pumping of spin waves by traveling acoustic waves has been examined both experimentally and theoretically in bulk magnetostrictive media^{8–11} and in infinitesimally thin films¹⁸. Recently, the parametric pumping of BVSW by bulk acoustic waves has been demonstrated in ferromagnetic films¹⁹, proving the feasibility of spin waves parametric pumping via magnetostriction. We note here that elastic waves have also been successfully employed to excite ferromagnetic resonance and traveling spin-waves in a linear regime^{20–22}.

Typical dimensions of spin-wave devices employing electromagnetic pumping are much smaller than the electromagnetic wavelength, thus the phase of the pumping electromagnetic field is practically uniform across the pumping region. Therefore the pumping electromagnetic waves are always “seen” as stationary by spin-waves^{6,15}. On the other hand, acoustic waves wavelengths are on the same order as typical spin waves localization in modern magnonic and spintronic devices^{16,23–26}. The small wavelength of the acoustic waves allows studying parametric pumping of spin-waves by traveling waves.

In this work, we develop a general theory of parametric interaction of acoustic waves and *localized* spin waves with arbitrary distribution of the displacement field in the acoustic wave and arbitrary spin-wave mode. Employing the theory, we show a possibility of parametric instabilities in FVSWs, confined in a spin-wave waveguide, generated by Rayleigh surface acoustic waves (SAW). The instabilities can be either convective or absolute, for oblique or normal incidence of the SAW, respectively. The absolute instability leads to generation of FVSW by SAW. For convective instability, by selecting a critical incident angle one can achieve a regime when spin-waves are amplified without generating a counter-propagating wave (idler), increasing the amplification efficiency. In yttrium iron garnet (YIG), a commonly used magnetostrictive ferrimagnet, the thresholds of the SAW strain amplitude for convective and absolute instabilities are less than ≈ 45 ppm, which within the maximum experimentally achievable strain²⁷.

II. PARAMETRIC COUPLING BETWEEN ACOUSTIC AND SPIN-WAVES

Theories for parametric magneto-elastic interactions^{18,28,29} developed in the past focused on waves in bulk samples, i.e. the localization of spin-waves was not considered. Here we develop a theory that captures the physics of parametric interactions in a case of localized spin-waves in samples with an arbitrary direction of the magnetization and acoustic wave modes with an arbitrary distribution of the strain field.

At first, we consider the dynamics of magnetization vector $\mathbf{M}(t, \mathbf{r})$ in a ferromagnetic sample without any deformation. This dynamics is governed by the Landau-

Lifshitz equation¹²:

$$\frac{d\mathbf{M}(t, \mathbf{r})}{dt} = \gamma \mathbf{B}^{\text{eff}}(t, \mathbf{r}) \times \mathbf{M}(t, \mathbf{r}), \quad (1)$$

where \mathbf{B}^{eff} is an effective magnetic field acting on the sample, including bias fields, shape and crystalline anisotropy. Restricting analysis to small angle precession dynamics (non-linear terms can be added later in a same fashion as in [30]), we expand the magnetization $\mathbf{M}(t, \mathbf{r})$ into the static and dynamic part:

$$\mathbf{M}(t, \mathbf{r}) = M_s(\boldsymbol{\mu}(\mathbf{r}) + \mathbf{s}(t, \mathbf{r})), \quad (2)$$

where M_s is the saturation magnetization, $\boldsymbol{\mu}(\mathbf{r})$ is the unit vector pointing the direction of equilibrium magnetization (ground state vector) and $\mathbf{s}(t, \mathbf{r})$ is the spin waves excitation vector. In an absence of the high order anisotropy, the Landau-Lifshitz equation can be linearized by substituting (2) into (1)^{12,30–33}:

$$\hat{\mathbf{J}}(\mathbf{r}) \cdot \frac{d\mathbf{s}(t, \mathbf{r})}{dt} = \int \hat{\boldsymbol{\Omega}}(\mathbf{r}, \mathbf{r}') \cdot \mathbf{s}(t, \mathbf{r}') d^3\mathbf{r}', \quad (3)$$

where $\hat{\mathbf{J}}(\mathbf{r}) = \hat{\mathbf{e}} \cdot \boldsymbol{\mu}(\mathbf{r})$ is the angular momentum operator removing all components parallel to the static magnetization direction which are irrelevant to the magnetization dynamics, $\hat{\mathbf{e}}$ is the Levi-Civita operator, $\hat{\boldsymbol{\Omega}}(\mathbf{r}, \mathbf{r}')$ is the Hamiltonian expressed in the frequency units of energy^{30–32}:

$$\hat{\boldsymbol{\Omega}}(\mathbf{r}, \mathbf{r}') = \gamma B \hat{\mathbf{I}} \delta(\mathbf{r} - \mathbf{r}') + \gamma \hat{\mathbf{P}}(\mathbf{r}) \cdot \hat{\mathcal{D}}(\mathbf{r}, \mathbf{r}') \cdot \hat{\mathbf{P}}(\mathbf{r}'), \quad (4)$$

$\hat{\mathcal{D}}(\mathbf{r}, \mathbf{r}')$ is the self-adjoint operator describing the self-interactions in the ferromagnet *without any deformations*, $\hat{\mathbf{P}}(\mathbf{r}) = -\hat{\mathbf{J}}(\mathbf{r}) \cdot \hat{\mathbf{J}}(\mathbf{r})$ is the projector, $\hat{\mathbf{I}}$ is an identity matrix, γ is the gyromagnetic ratio, and B is the modulus of the internal magnetic field. The modulus of the internal magnetic field, B , and the ground state vector $\boldsymbol{\mu}(\mathbf{r})$, entering (3), can be found from the “static” part of the Landau-Lifshitz equation:

$$\boldsymbol{\mu}(\mathbf{r})B = \mathbf{B}^{\text{ext}}(\mathbf{r}) - \int \hat{\mathcal{D}}(\mathbf{r}, \mathbf{r}') \cdot \boldsymbol{\mu}(\mathbf{r}') d^3\mathbf{r}', \quad (5)$$

See Supplementary Material on Ref. 30 for more details of this formalism. Additionally, higher order anisotropy terms can be introduced in a similar manner as in [31].

Here Eq. (3) is a generalized eigen-value problem, thus its solutions can written as:

$$\mathbf{s}(t, \mathbf{r}) = \sum_{\nu} c_{\nu} e^{-i\omega_{\nu} t} \mathbf{s}_{\nu}(\mathbf{r}) + \text{c.c.}, \quad (6)$$

where c_{ν} is the dimensionless complex amplitude of ν -th mode. Here the eigen-modes $\mathbf{s}_{\nu}(\mathbf{r})$ form an orthogonal basis with an orthogonality condition^{30,33}:

$$\int \mathbf{s}_{\nu}^{\dagger}(\mathbf{r}) \cdot \hat{\mathbf{J}}(\mathbf{r}) \cdot \mathbf{s}_{\nu'}(\mathbf{r}) d^3\mathbf{r} = -iA_{\nu} \delta_{\nu\nu'}, \quad (7)$$

where $\mathcal{A}_\nu > 0$ is the mode norm, \dagger denotes Hermitian conjugation, and $\delta_{\nu,\nu'}$ is the Kronecker symbol.

A deformation of a magnetic material changes the energy density, \mathcal{W} , of the magnetic subsystem by the value

$$\mathcal{W}_{\text{me}}(t, \mathbf{r}) = \frac{1}{M_s^2} b_{ijkl} U_{ij}(t, \mathbf{r}) \mathbf{M}_k \mathbf{M}_l, \quad (8)$$

where $U_{ij}(t, \mathbf{r})$ is the induced strain, b_{ijkl} is the tensor of magnetostriction, $ijkl = \{x, y, z\}$, and repetitive indices indicate summation. The effect of the strain can be introduced into (3)–(5) as a perturbation to the self-interaction operator

$$\delta \hat{\mathcal{D}}(t, \mathbf{r}, \mathbf{r}') = \frac{2}{M_s} b_{ijkl} U_{ij}(t, \mathbf{r}) \delta(\mathbf{r} - \mathbf{r}') = a(t) \hat{\mathbf{T}}(\mathbf{r}) \delta(\mathbf{r} - \mathbf{r}') + \text{c.c.}, \quad (9)$$

where $U_{ij}(t, \mathbf{r}) = a(t) u_{ij}(\mathbf{r}) + \text{c.c.}$, $a(t)$ and $u_{ij}(\mathbf{r})$ are a dimensionless complex amplitude and the complex mode profile of the acoustic wave, and $\hat{\mathbf{T}}(\mathbf{r}) = 2b_{ijkl} u_{ij}(\mathbf{r}) / M_s$. Here the operator $\hat{\mathbf{T}}(\mathbf{r})$ can be seen as a tensor for an effective magnetic anisotropy generated by the acoustic field. Substituting the perturbation (9) into (5) and multiplying by $\boldsymbol{\mu}(\mathbf{r})$ we find the time-dependent correction to the internal magnetic field (we assume that the strain has no static component):

$$\delta B(t, \mathbf{r}) = -a(t) \boldsymbol{\mu}(\mathbf{r}) \cdot \hat{\mathbf{T}}(\mathbf{r}) \cdot \boldsymbol{\mu}(\mathbf{r}) + \text{c.c.} \quad (10)$$

Adding perturbation to (3) leads to:

$$\hat{\mathcal{J}}(\mathbf{r}) \cdot \frac{d\mathbf{s}(t, \mathbf{r})}{dt} = \int \hat{\boldsymbol{\Omega}}(\mathbf{r}, \mathbf{r}') \cdot \mathbf{s}(t, \mathbf{r}') d^3 \mathbf{r}' + \gamma \delta B(t, \mathbf{r}) \mathbf{s}(t, \mathbf{r}) + [a(t) \hat{\mathbf{T}}(\mathbf{r}) + \text{c.c.}] \cdot \mathbf{s}(t, \mathbf{r}) + [a(t) \hat{\mathbf{T}}(\mathbf{r}) \cdot \boldsymbol{\mu}(\mathbf{r}) + \text{c.c.}] \quad (11)$$

We solve the perturbed equation (11) by substituting $\mathbf{s}(t, \mathbf{r}) = \sum_\nu c_\nu(t) \mathbf{s}_\nu(\mathbf{r}) + \text{c.c.}$ and multiplying by $\mathbf{s}_{\nu'}^\dagger(\mathbf{r})$. Using the condition (7) and retaining only “parametric” terms⁶ we obtain:

$$\frac{dc_\nu(t)}{dt} + i\omega c_\nu(t) + \Gamma_\nu c_\nu(t) = a(t) \sum_{\nu'} V_{\nu\nu'} c_{\nu'}^\dagger(t), \quad (12)$$

where Γ_ν is the phenomenological damping term and $V_{\nu\nu'}$ is the coupling coefficient, which can be calculated as:

$$V_{\nu\nu'} = V_{\nu\nu'}^1 + V_{\nu\nu'}^2 = -i \frac{\gamma}{\mathcal{A}_\nu} \int (\mathbf{s}_{\nu'}^\dagger(\mathbf{r}) \cdot \mathbf{s}_\nu^\dagger(\mathbf{r})) (\boldsymbol{\mu}(\mathbf{r}) \cdot \hat{\mathbf{T}}(\mathbf{r}) \cdot \boldsymbol{\mu}(\mathbf{r})) d^3 \mathbf{r} + i \frac{\gamma}{\mathcal{A}_\nu} \int (\mathbf{s}_{\nu'}^\dagger(\mathbf{r}) \cdot \hat{\mathbf{T}}(\mathbf{r}) \cdot \mathbf{s}_\nu^\dagger(\mathbf{r})) d^3 \mathbf{r}. \quad (13)$$

This expression is the central result of this work, it enables one to calculate the parametric coupling between

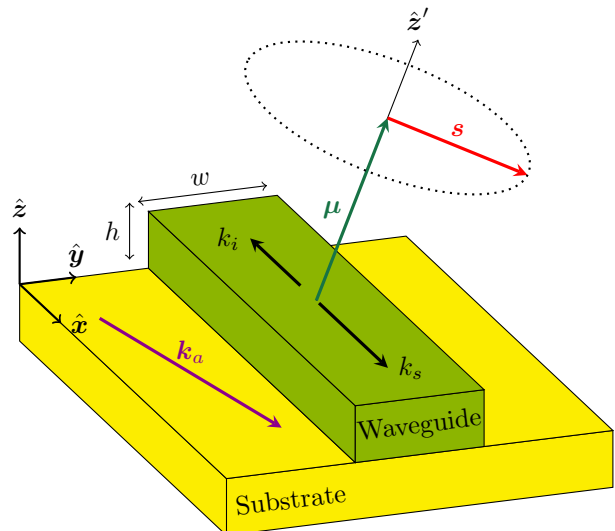


FIG. 1. Sketch showing the geometry of the confined spin-wave waveguide located on a substrate.

arbitrary spin-waves and acoustic waves. Using this result with the well developed theory of parallel pumping^{4,6,15,16}, we can investigate the dynamics of spin-waves under acoustic pumping.

The mode profiles in (13) (the distribution of magnetization $\mathbf{s}(\mathbf{r})$ for spin-waves and the distribution of strain $\hat{\mathbf{u}}(\mathbf{r})$ for acoustic waves) can be calculated either analytically or extracted from numerical simulations for acoustic waves and spin waves. Importantly, we have not used an explicit form of the self-interaction operator $\hat{\mathcal{D}}(\mathbf{r}, \mathbf{r}')$. Thus the presented theory is not restricted to a particular configuration of the problem, i.e. a direction of the equilibrium magnetization, a specific type of an acoustic wave, or a particular geometry of the magnetic sample, as was the case in previous methods^{8,18,34,35}.

We note also, that a general expression similar to (13), but for linear magneto-elastic interactions has been obtained in Ref. [36].

III. SELECTION RULES AND A MOMENTUM CONSERVATION LAW

To discuss the physical meaning of the terms entering the coupling coefficient, $V_{\nu\nu'}$, we consider a simple case: a rectangular magnetic waveguide placed atop of a solid non-magnetic substrate, see Fig. 1. The waveguide is infinite in the \hat{x} direction and constrained in the \hat{y} and \hat{z} directions. The width of the waveguide is w and the height is h . The magnetic waveguide is uniformly magnetized with the magnetic ground state $\boldsymbol{\mu}$.

The spin-waves can travel along x -direction in the waveguide and are constrained in the y and z directions, see Fig. 1. In this situation we consider interaction of three waves: two spin-waves having wave-numbers k_s and k_i (traditionally termed as “signal” and “idler” waves),

and an acoustic wave propagating in the x, y plane with wavevector \mathbf{k}_a , see Fig. 1

A spin excitation vector for each wave (signal and idler) can be written as:

$$\mathbf{s}_k = \tilde{\mathbf{s}}_k f_k(y, z) e^{ikx}, \quad (14)$$

where $k = k_s, k_i$, $f_k(y, z)$ is the spin-wave mode profile across the waveguide, i.e. the distribution of the spin-wave mode amplitude within the waveguide, and $\tilde{\mathbf{s}}_k$ is the polarization of the spin-wave mode. The polarization $\tilde{\mathbf{s}}_k$ depends on the direction of the equilibrium magnetization $\boldsymbol{\mu}$ and ellipticity of precession. In a coordinate system where the z' axis is oriented with the equilibrium magnetization ($\boldsymbol{\mu} = \hat{z}'$) the polarization can be written as, see Fig. 1:

$$\tilde{\mathbf{s}}'_k = \begin{pmatrix} 1 \\ i\epsilon_k \\ 0 \end{pmatrix}, \quad (15)$$

where ϵ_k is the ellipticity of the precession. For simplicity we take the ellipticity to not depend on the spatial coordinates in the waveguide. The mode norm can be calculated as:

$$\mathcal{A}_k = 2\epsilon_k \iint_S |f_k(y, z)|^2 dydz = 2\epsilon_k \mathcal{A}_k^S, \quad (16)$$

where S is the cross-sectional area of the waveguide, see Fig. 1.

Let us also choose that the acoustic wave is uniform in the whole space and propagates in the plane of the waveguide

$$u_{ij} = \tilde{u}_{ij} e^{i\mathbf{k}_a \cdot \mathbf{r}} = \tilde{u}_{ij} e^{i(k_{||}x + k_{\perp}y)}, \quad (17)$$

where $k_{||}$ and k_{\perp} are the projections of the acoustic wavevector on the x and y axes, respectively.

Substituting the assumed mode profiles into (13) we have

$$V_{k_s, k_i} = \gamma (\tilde{V}_{k_s, k_i}^1 + \tilde{V}_{k_s, k_i}^2) F_{k_s, k_i} \delta(k_s + k_i - k_{||}) \quad (18)$$

where

$$F_{k_s, k_i} = \frac{1}{\mathcal{A}_{k_s}^S} \iint_S f_{k_s}(y, z) f_{k_i}(y, z) e^{ik_{\perp}y} dydz \quad (19)$$

is the overlap integral between two spin-waves and one acoustic wave.

The delta-function in (18) postulates a momentum conservation law:

$$k_s + k_i = k_{||}, \quad (20)$$

This conservation law is modified in the comparison to the bulk case²⁹, $\mathbf{k}_s + \mathbf{k}_i = \mathbf{k}_a$, i.e. when the spin-waves are not localized in the waveguide. In the localized case the translational symmetry holds in the x -direction

and breaks in the y -direction. Therefore, as a consequence of Noether's theorem, the x -component of momentum is conserved for three interacting waves, but the y -component is not. The momentum conservation law acts as a selection rule, defining the wave-numbers of the interacting spin-waves.

The expression (20) corresponds to the case of the electromagnetic-like spin wave pumping^{4,6} when the acoustic wave has no x -component $k_{||} = 0$, and to the "optical"-like co-propagating wave pumping¹ for $\mathbf{k}_a = k_{||} \hat{x}$.

The overlap integral, F_{k_s, k_i} , contains profiles of both spin-waves and an oscillating function $e^{ik_{\perp}y}$. The overlap integral defines another selection rule for interacting spin-waves, based on the precession amplitude spatial distribution $f_{k_s}(y, z)$ and $f_{k_i}(y, z)$. In general, calculation of mode spatial profiles is non-trivial and frequently requires numerical solutions. However, under reasonable assumptions we can analyze the behavior of the overlap integral analytically. If the cross-section distribution of both waves is uniform, $f_{k_s}(y, z) = f_{k_i}(y, z) = 1$, the overlap integral can be easily calculated as

$$F_{k_s, k_i} = \frac{\sin(k_{\perp}w/2)}{k_{\perp}w/2}. \quad (21)$$

From the above equation, one can conclude that the coupling coefficient drops with the width of the waveguide and the parametric interaction becomes inefficient when $w \gg 1/k_{\perp}$.

In the case of thin waveguides, $h \ll w$, (see Fig. 1) we can consider $f_k(y, z)$ as harmonic functions depending on y coordinate³⁷⁻³⁹. Here we consider two practically important cases, when the magnetization is pinned or unpinned at the waveguide boundaries in the y direction. Also, we assume that the profiles are identical for signal and idler waves, $f_{k_s}(y, z) = f_{k_i}(y, z) = f_k(y, z)$. Thus, the spatial profiles can be written as:

$$\begin{aligned} f_k &= \cos\left(\frac{\pi N(y + w/2)}{w}\right) \quad \text{for unpinned,} \\ f_k &= \sin\left(\frac{\pi N(y + w/2)}{w}\right) \quad \text{for pinned,} \end{aligned} \quad (22)$$

where $N = 1, 2, \dots$ is the mode number. Substituting the expressions for spatial profiles into (19) we find expressions for the overlap integral in two cases:

$$F_{kk}^u = \frac{4(2N^2\pi^2 - k_{\perp}^2 w^2) \sin(k_{\perp}w/2)}{4\pi^2 k_{\perp} w N^2 - k_{\perp}^3 w^3} \quad \text{for unpinned,} \quad (23)$$

$$F_{kk}^p = \frac{8N^2\pi^2 \sin(k_{\perp}w/2)}{4\pi^2 k_{\perp} w N^2 - k_{\perp}^3 w^3} \quad \text{for pinned.} \quad (24)$$

Similar to (21), these functions have a global maximum at $k_{\perp}w \rightarrow 0$. However they also exhibit a local maximum at $w = 2\pi N/k_{\perp}$: $F_{kk}^u = F_{kk}^p = \pm 1/2$, allowing for interaction of high order modes, $N > 0$, in wide waveguides $w > 1/k_{\perp}$.

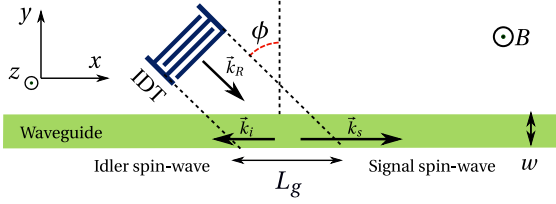


FIG. 2. Top view of a setup for spin-wave surface acoustic wave parametric interaction. A Rayleigh surface acoustic wave propagates in the substrate, while a spin-wave propagates in the magnetic waveguide (green). The magnetic field \mathbf{B} is applied perpendicular to the plane.

Finally, we consider terms of \tilde{V}_{k_s, k_i}^1 and \tilde{V}_{k_s, k_i}^2 . These terms define selection rules based on the vector structure of the magnetization precession, elastic deformations, and magnetostrictive tensor b_{ijkl} . The first term can be written in a form:

$$\tilde{V}_{k_s, k_i}^1 = -i \frac{1 - \epsilon^2}{2\epsilon} \tilde{b}_p, \quad (25)$$

where we consider the ellipticity of both idler and signal spin-waves to be identical $\epsilon_{k_s} = \epsilon_{k_i} = \epsilon$. The term $\tilde{b}_p = \boldsymbol{\mu} \cdot \hat{\mathbf{T}} \cdot \boldsymbol{\mu}$ with $\hat{\mathbf{T}} = b_{ijkl} \tilde{u}_{ij}$ describes the projection of an effective magnetic field, generated by the inverse magnetostriction effect on the direction of the static magnetization. The symmetry of the term \tilde{V}_{k_s, k_i}^1 is identical to the symmetry of the coupling coefficient to an RF magnetic field for the parallel pumping mechanism¹². Therefore this term vanishes for spin-wave having circular precession, i.e. $\epsilon = 1$.

The second term \tilde{V}_{k_s, k_i}^2 is different: here, the operator $\hat{\mathbf{T}}$ acts directly on the spin-waves mode profiles and the coupling coefficient can be non-zero even for the modes having circular precession:

$$\tilde{V}_{k_s, k_i}^2 = i \frac{\mathbf{s}_{k_s} \cdot \hat{\mathbf{T}} \cdot \mathbf{s}_{k_i}}{2\epsilon_k}. \quad (26)$$

The particular form of this term depends on the deformation introduced by the acoustic wave and the symmetry of the tensor of magnetostriction. Physically this

term represents perturbations of the precession trajectory made by the modulation of the effective magnetic anisotropy. We note here that similar terms were obtained for the parametric pumping of spin waves with voltage-controlled magnetic anisotropy^{40,41}.

IV. INTERACTION BETWEEN SURFACE ACOUSTIC WAVES AND FORWARD VOLUME SPIN-WAVES

As an illustration for our theory we calculate the parametric interactions between forward volume spin waves traveling in a YIG waveguide and a Rayleigh SAW traveling in the GGG substrate (velocity $c_R \approx 5$ km/s), see Fig. 2. The parameters for YIG are taken as follows: Saturation magnetization¹² is $M_s = 135$ kA/m, exchange constant⁴² $A_{\text{ex}} = 3.7$ fJ/m, magnetostrictive tensor components for a cubic crystal¹² $b_{iiii} = B_1 = 0.35$ MJ/m³ and $b_{ijij} = B_2 = 0.7$ MJ/m³, $i \neq j$, damping decrement $\Gamma/(2\pi) = \gamma\delta H/2 = 1.5$ MHz.

Calculation of the acoustic field in an YIG waveguide placed atop a substrate is non-trivial³⁴. To simplify our analytical calculations, we will consider a thin and narrow ferromagnetic waveguide with $h \ll \lambda_R$ and $w < L_g$ where the $\lambda_R = 2\pi k_R$ is the SAW wavelength, k_R is the SAW wave-number, h is the thickness, w is the width and L_g is the length of the interaction region, see Fig. 2. Also for simplicity, we assume the strain to be uniformly distributed in the waveguide and equal to the surface strain created by the SAW⁴³, and the substrate to be isotropic. Thus, the acoustic mode has the form $\hat{\mathbf{u}} = (\mathbf{k}_R \otimes \mathbf{k}_R / k_R^2 + i u_{zz} \mathbf{z} \otimes \mathbf{z}) e^{i\mathbf{k}_R \cdot \mathbf{r}}$, where u_{zz} is the ratio between the vertical and lateral stress. We also consider the pumping to be coherent in time as $a(t) = a e^{-i\omega_p t}$.

Spin waves modes in perpendicular magnetized waveguides are typically pinned to the lateral edges. The spin excitation vector for the fundamental mode can be written as: $\mathbf{s}_k = (\hat{\mathbf{x}} + i\epsilon_k \hat{\mathbf{y}}) \sin(\pi y/w) e^{ikx - i\omega t}$, where ϵ is the precession ellipticity, and the precession is almost circular ($|1 - |\epsilon_k|| \ll 1$) for perpendicularly magnetized samples and small k .

First we consider a case of an infinitely long pumping region, L_g . Using the above described formalism in Sec. III into (13) we obtain expressions of the coupling coefficient between the signal and idler waves:

$$V_{k_s, k_i} = V_0(\phi) = \frac{\gamma B_1}{M_s} \frac{(\cos \phi - i\epsilon_k \sin(\phi))^2 - i u_{zz} (1 - \epsilon_k^2)}{2\epsilon_k} F_{kk}^p \delta(k_s + k_i - k_R \sin \phi) \approx \frac{\gamma B_1}{2M_s} F_{kk}^p \delta(k_s + k_i - k_R \sin \phi) e^{i\phi}. \quad (27)$$

The factor $V_0(\phi)$ defines the “strength” of the parametric interaction. The modulus of $V_0(\phi)$ is plotted in

Fig. 3(a) for parameters of YIG. A parametric instability in an waveguide with an infinitely long pumping region

occurs when pumping overcomes the damping in the system. The threshold amplitude of the SAW is defined by the expression (assuming that ω_{k_s} and ω_{k_i} fall within the spin waves spectra):

$$|a_{\text{th}}(\phi)| = \Gamma/|V_0(\phi)|, \quad (28)$$

where Γ is the damping decrement of the fundamental mode. For $\phi = \pi/2$, i.e. when all three waves travel colinearly, the threshold value is equal to the threshold value obtained ignoring the spin-wave localization^{12,18}. For the selected parameters the threshold value is $|a_{\text{th}}^{\text{min}}| \approx 21$ ppm, which is lower than the typical failure strain (300 ppm) of Al transducers²⁷. If $\phi \neq \pi/2$, the existence of the spin-wave localization increases the threshold for the spin-wave instability. The particular type of the instability (absolute or convective, in other words, developing in time or space respectively) is defined by the relative signs of the group velocities $v_{\text{gr}}(k_s)$ and $v_{\text{gr}}(k_i)$ ⁶.

The threshold (28) is directly proportional to the damping in the magnetic material and inversely proportional to the coefficient to magnetostriction. Therefore, it is feasible to consider materials with higher damping rates, but, at the same time, stronger magneto-elastic interaction, as a substitute for YIG. For example, recently, linear^{44–46} and parametric⁴⁷ magneto-elastic interactions have been observed in relatively lossy Ni films. Using (28) and parameters for Ni films³⁶ ($\alpha_G = 0.045$, $B_1 \approx B_2 \approx 10$ MJ/m³, $\mu_0 M_s = 0.66$ T, $\omega/(2\pi) = 1.5$ GHz) we can estimate the strain threshold as $|a_{\text{th}, \text{Ni}}^{\text{min}}| \approx 260$ ppm, which is at the limit of the commonly used Al SAW transducers, but easily obtainable with optical techniques of SAW excitation^{46,48}.

V. PARAMETRIC INSTABILITIES IN A SPATIALLY LIMITED PUMPING REGION

Experimentally, the pumping region is always limited in space. A localized pumping region increases the threshold for absolute instabilities and prevents development of convective instabilities^{15,49}. Absolute instabilities lead to generation of detectable spin-waves from thermal fluctuations, which is often is a problem in amplifiers and active delay lines, where the parasitic generation can cause undesired cross-talk. On the other hand, a special case of convective instability when the group velocity of the idler wave becomes zero is important for spin waves amplifiers. Since the idler then cannot “leak” outside the pumping region the parametric interaction is very effective⁴⁹. Such a situation is difficult to implement for electromagnetic pumping, because the frequency and group velocities for both signal and idler spin-waves are the same. For acoustic pumping, the modified momentum conservation law (20) allows parametric interaction of spin waves with different wave-numbers and, as a consequence, with different frequencies, $\omega_{k_s} \neq \omega_{k_i}$

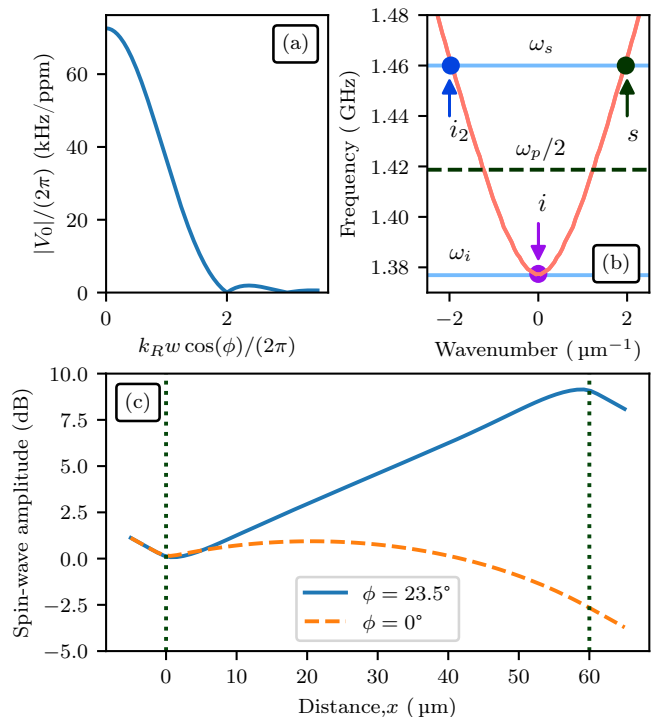


FIG. 3. a) Parametric interaction coefficient V_0 for the surface acoustic waves and spin-waves in a rectangular waveguide as function of the waveguide width w and the projection of the SAW wave-vector perpendicular to the waveguide k_\perp ; b) Numerically calculated spin-wave spectrum in a rectangular YIG waveguide; c) Amplitude of spin-waves under a parametric pumping for an oblique incident acoustic waves (blue, solid) and perpendicular SAW (orange, dashed), vertical dotted lines enclose the pumping region. The amplitude of the strain in the acoustic wave is selected as $a = 31$ ppm $> a_{\text{th}}(\phi)$. See text for the parameters of the waveguide and materials.

and $\omega_{k_s} + \omega_{k_i} = \omega_p$. To achieve a convective instability we select the idler wave with a zero group velocity $v_{\text{gr}}(k_i) = 0$ at $k_i = 0$. Thus for a signal wave with the frequency ω_s the pumping frequency is $\omega_p = \omega_s + \omega_{k_i=0}$ and $\sin \phi = k_s/k_R$.

In our example we take the waveguide with geometrical parameters $h = 100$ nm and $w = 1$ μm , which can be fabricated experimentally⁵⁰, and the interaction region is length $L_g = 60$ μm , see Fig. 2. The spin waves spectrum in the waveguide biased by normal magnetic field $B = 20$ mT shown in Fig. 3(b). Since the waveguide is limited in the lateral direction, the spin wave group velocity drops with the wave-number approaching zero. The spectrum was calculated numerically using MuMax³ micromagnetics simulator⁵¹.

We select the signal frequency $\omega_s/(2\pi) = 1.46$ GHz, which corresponds to $k_s \approx 2$ μm^{-1} (marked by symbol s in Fig. 3(b)). The spectrum minimum with $k = 0$ corresponds to the frequency $\omega_i = 1.37$ GHz (symbol i in Fig. 3(b)). To satisfy the conservation laws we select the pumping frequency $\omega_p \approx 2.48$ GHz, see Fig. 3(b). To satisfy (20) we shall select an appropriate incident angle

$\phi_0 \approx 23.5^\circ$. The parametric coefficient for this angle is $V_0(\phi_0) \approx 50$ kHz/ppm.

We use a standard “slow envelope” technique to find the spin waves amplitude distribution^{4,6,15}. However, in our case, the group velocity of the idler spin waves vanishes, thus we need to take into account the spin-wave diffusion of the idler waves⁴⁹:

$$\begin{aligned} v_{\text{gr}} \frac{db_s(x)}{dx} + \Gamma b_s(x) &= V_0 \theta_P(x) b_i^\dagger(x) a, \\ i \frac{D}{2} \frac{d^2 b_i^\dagger(x)}{dx^2} + \Gamma b_i^\dagger(x) &= -V_0^\dagger \theta_P(x) b_s(x) a \end{aligned} \quad (29)$$

where $b_{s,i}(x)$ are the amplitudes of the signal and idler envelopes (see Ref. 15 for definition), $v_{\text{gr}} \approx 0.38$ km/s is the group velocity of the signal wave, $D = d^2\omega_k/dk^2 \approx 2.24$ cm²/s is the diffusion coefficient, and $\theta_P(x)$ is a function which equals 1 inside the interaction region and 0 otherwise. The values of D and v_{gr} were calculated numerically using MuMaX³.

The amplitude of the signal wave found by a numerical solution of (29) is plotted in Fig. 3(c) in the blue line for the in-plane SAW strain amplitude $a_0 = 31$ ppm. This value is above the threshold (28) and the energy coming from the acoustic wave overcomes damping in the system. The amplitude of the signal and idler (not shown) waves exponentially increases in the $x > 0$ direction. The growth of the amplitude is limited by the finite length of the interaction region.

The induced idler wave can interact, in its turn, with a “secondary” idler wave with frequency ω_s and the wave-number $-k_s$, marked as i_2 in Fig. 3(b). This interaction, however, can be effective only in a non-adiabatic case⁶ $k_s L_g \ll 1$. For the considered geometry this interaction is negligibly small.

The dashed orange line in Fig. 3(c) represents a solution for a normally incident SAW ($\phi = 0$). In this

case both signal and idler waves have the same frequency ($\omega_p/2 \times 1/(2\pi) \approx 1.42$ GHz) and group velocity $v_{\text{gr}} \approx 0.38$ km/s. In order to make a comparison with the previous case we increase the pumping amplitude $a_1 = 34$ ppm to compensate the drop in the pumping efficiency. Now the idler wave “leaks” out of the interaction region, and the spin-waves cannot be effectively amplified⁶. Therefore, the amplitude of the signal spin wave at the end of the pumping region is more than ten times less than in the oblique SAW case. We want to emphasize, that the difference in the spin-wave output coming not from greater parametric coupling with the SAW, but because the group velocity of the idler spin-wave is zero.

However, in the case of $\phi = 0$ an absolute instability is possible with a threshold acoustic amplitude $a_{\text{th}} \approx 45$ ppm for $L_g = 60$ μm . After exceeding this threshold, thermal fluctuations are pumped and increase their amplitudes exponentially.

VI. CONCLUSION

We developed a perturbation theory of parametric interaction between localized spin-waves and acoustic waves. With the theory we demonstrated that: i) the localization of spin-waves modifies the momentum conservation law for parametric pumping, ii) the symmetry of the magneto-elastic coupling allows an efficient interaction between the Rayleigh surface acoustic waves and forward volume spin-waves having circular precession, and iii) both convective and absolute parametric instabilities can develop for spin-waves under experimentally achievable amplitudes of surface acoustic waves, which results in efficient amplification of spin waves in ferromagnetic waveguides.

The work was supported by the United States Defense Advanced Research Projects Agency (DARPA) Signal Processing at RF (SPAR) grant HR0011-17-2-0005.

* Now with Winchester Technologies, LLC, Burlington, MA; <https://www.lisenkov.com>; ivan@lisenkov.com

¹ Nicolaas Bloembergen, *Nonlinear Optics (4th Edition)* (World Scientific Publishing Company, 1996).

² N. S. Erokhin, V. E. Zakharov, and S. S. Moiseev, “Second Harmonic Generation by an Electromagnetic Wave Incident on Inhomogeneous Plasma,” *Soviet Journal of Experimental and Theoretical Physics* **29**, 101 (1969).

³ Marcel Lesieur, *Turbulence in Fluids (Fluid Mechanics and Its Applications)* (Springer, 2014).

⁴ Victor S. L’vov, *Wave Turbulence Under Parametric Excitation: Applications to Magnets (Springer Series in Nonlinear Dynamics)* (Springer-Verlag, 1994).

⁵ Vladimir E. Zakharov, Victor S. L’vov, and Gregory Falkovich, *Kolmogorov Spectra of Turbulence I: Wave Turbulence (Springer Series in Nonlinear Dynamics) (v. 1)* (Springer, 1992).

⁶ G. A. Melkov, A. A. Serga, V. S. Tiberkevich, Yu. V. Kobljanskij, and A. N. Slavin, “Nonadiabatic interaction

of a propagating wave packet with localized parametric pumping,” *Physical Review E* **63** (2001), 10.1103/physreve.63.066607.

⁷ Max Born and Emil Wolf, *Principles of optics : electromagnetic theory of propagation, interference and diffraction of light* (Cambridge University Press, Cambridge New York, 1999).

⁸ H. Matthews and F. R. Morgenthaler, “Phonon-pumped spin-wave instabilities,” *Physical Review Letters* **13**, 614–616 (1964).

⁹ B. A. Auld and H. Matthews, “Parametric traveling-wave acoustic amplification in ferromagnets,” *Journal of Applied Physics* **36**, 3599–3605 (1965).

¹⁰ C. Warren Haas, “Amplification of spin waves by phonon pumping,” *Journal of Physics and Chemistry of Solids* **27**, 16871695 (1966).

¹¹ Donald H. Lyons and H. Matthews, “Parametric excitation of spin waves by phonon pumping,” *Journal of Applied Physics* **44**, 1348–1355 (1973).

- ¹² Alexander G. Gurevich and Gennadii A. Melkov, *Magnetization Oscillations and Waves* (CRC Press, 1996).
- ¹³ E. Schlömann, J. J. Green, and U. Milano, “Recent developments in ferromagnetic resonance at high power levels,” *Journal of Applied Physics* **31**, S386–S395 (1960).
- ¹⁴ V. V. Zautkin, V. E. Zakharov, V. S. L’Vov, S. L. Musher, and S. S. Starobinets, “Parallel Spin-wave Pumping in Yttrium Garnet Single Crystals,” *Soviet Journal of Experimental and Theoretical Physics* **35**, 926 (1972).
- ¹⁵ G. A. Melkov, A. A. Serga, A. N. Slavin, V. S. Tiberkevich, A. N. Oleinik, and A. V. Bagada, “Parametric interaction of magnetostatic waves with a nonstationary local pump,” *Journal of Experimental and Theoretical Physics* **89**, 1189–1199 (1999).
- ¹⁶ T. Brächer, P. Pirro, and B. Hillebrands, “Parallel pumping for magnon spintronics: Amplification and manipulation of magnon spin currents on the micron-scale,” *Physics Reports* (2017), 10.1016/j.physrep.2017.07.003.
- ¹⁷ Yu. V. Kobljanskyj, G. A. Melkov, A. A. Serga, V. S. Tiberkevich, and A. N. Slavin, “Effective microwave ferrite convolver using a dielectric resonator,” *Applied Physics Letters* **81**, 16451647 (2002).
- ¹⁸ Hedyeh Keshtgar, Malek Zareyan, and Gerrit E.W. Bauer, “Acoustic parametric pumping of spin waves,” *Solid State Communications* **198**, 30–34 (2014).
- ¹⁹ Pratim Chowdhury, Albrecht Jander, and Pallavi Dhagat, “Nondegenerate parametric pumping of spin waves by acoustic waves,” *IEEE Magnetics Letters* **8**, 1–4 (2017).
- ²⁰ L. Thevenard, I. S. Camara, J.-Y. Prieur, P. Rovillain, A. Lemaître, C. Gourdon, and J.-Y. Duquesne, “Strong reduction of the coercivity by a surface acoustic wave in an out-of-plane magnetized epilayer,” *Physical Review B* **93** (2016), 10.1103/PhysRevB.93.140405.
- ²¹ L. Thevenard, I. S. Camara, S. Majrab, M. Bernard, P. Rovillain, A. Lemaître, C. Gourdon, and J.-Y. Duquesne, “Precessional magnetization switching by a surface acoustic wave,” *Physical Review B* **93** (2016), 10.1103/PhysRevB.93.134430.
- ²² Piotr Kuszewski, Jean-Yves Duquesne, Loic Becerra, Aristide Lemaître, Serge Vincent, Silbe Majrab, Florent Margailan, Catherine Gourdon, and Laura Thevenard, “Optical probing of Rayleigh wave driven magnetoacoustic resonance,” arXiv:1806.11410 [cond-mat] (2018), arXiv:1806.11410 [cond-mat].
- ²³ B. Hillebrands and K. Ounadjela, eds., *Spin Dynamics in Confined Magnetic Structures I (Topics in Applied Physics) (v. 1)* (Springer, 2001).
- ²⁴ A A Serga, A V Chumak, and B Hillebrands, “Yig magnonics,” *Journal of Physics D: Applied Physics* **43**, 264002 (2010).
- ²⁵ M. Collet, X. de Milly, O. d Allivy Kelly, V. V. Naletov, R. Bernard, P. Bortolotti, J. Ben Youssef, V. E. Demidov, S. O. Demokritov, J. L. Prieto, and et al., “Generation of coherent spin-wave modes in yttrium iron garnet microdiscs by spinorbit torque,” *Nature Communications* **7**, 10377 (2016).
- ²⁶ C. Safranski, I. Barsukov, H. K. Lee, T. Schneider, A. A. Jara, A. Smith, H. Chang, K. Lenz, J. Lindner, Y. Tserkovnyak, and et al., “Spin caloritronic nano-oscillator,” *Nature Communications* **8** (2017), 10.1038/s41467-017-00184-5.
- ²⁷ Y. Ebata and S. Mitobe, “A numerical method for stress analysis in a saw resonator,” 1998 IEEE Ultrasonics Symposium. Proceedings (Cat. No. 98CH36102) 10.1109/ultsym.1998.762140.
- ²⁸ C. Kittel, “Interaction of spin waves and ultrasonic waves in ferromagnetic crystals,” *Physical Review* **110**, 836–841 (1958).
- ²⁹ R. L. Comstock and B. A. Auld, “Parametric coupling of the magnetization and strain in a ferrimagnet. i. parametric excitation of magnetostatic and elastic modes,” *Journal of Applied Physics* **34**, 1461–1464 (1963).
- ³⁰ Oleksandr Dzyapko, Ivan Lisenkov, Patrik Nowik-Boltyk, Vladislav E. Demidov, Sergej O. Demokritov, Benny Koene, Andrei Kirilyuk, Theo Rasing, Vasyi Tiberkevich, and Andrei Slavin, “Magnon-magnon interactions in a room-temperature magnonic bose-einstein condensate,” *Physical Review B* **96** (2017), 10.1103/physrevb.96.064438.
- ³¹ Ivan Lisenkov, Vasyi Tyberkevych, Sergey Nikitov, and Andrei Slavin, “Theoretical formalism for collective spin-wave edge excitations in arrays of dipolarly interacting magnetic nanodots,” *Physical Review B* **93** (2016), 10.1103/physrevb.93.214441.
- ³² Roman Verba, Gennadiy Melkov, Vasil Tiberkevich, and Andrei Slavin, “Collective spin-wave excitations in a two-dimensional array of coupled magnetic nanodots,” *Physical Review B* **85** (2012), 10.1103/physrevb.85.014427.
- ³³ Roman Verba, Vasil Tiberkevich, and Andrei Slavin, “Damping of linear spin-wave modes in magnetic nanostructures: Local, nonlocal, and coordinate-dependent damping,” *Physical Review B* **98** (2018), 10.1103/PhysRevB.98.104408.
- ³⁴ Xu Li, Dominic Labanowski, Sayeef Salahuddin, and Christopher S. Lynch, “Spin wave generation by surface acoustic waves,” *Journal of Applied Physics* **122**, 043904 (2017).
- ³⁵ A. Barra, A. Mal, G. Carman, and A. Sepulveda, “Voltage induced mechanical/spin wave propagation over long distances,” *Applied Physics Letters* **110**, 072401 (2017).
- ³⁶ Roman Verba, Ivan Lisenkov, Ilya Krivorotov, Vasil Tiberkevich, and Andrei Slavin, “Nonreciprocal surface acoustic waves in multilayers with magnetoelastic and interfacial dzyaloshinskii-moriya interactions,” *Physical Review Applied* **9** (2018), 10.1103/physrevapplied.9.064014.
- ³⁷ J. Jorzick, S. O. Demokritov, B. Hillebrands, M. Bailleul, C. Fermon, K. Y. Guslienko, A. N. Slavin, D. V. Berkov, and N. L. Gorn, “Spin wave wells in nonellipsoidal micrometer size magnetic elements,” *Physical Review Letters* **88** (2002), 10.1103/physrevlett.88.047204.
- ³⁸ K. Y. Guslienko, R. W. Chantrell, and A. N. Slavin, “Dipolar localization of quantized spin-wave modes in thin rectangular magnetic elements,” *Physical Review B* **68** (2003), 10.1103/physrevb.68.024422.
- ³⁹ C. Bayer, J. Jorzick, B. Hillebrands, S. O. Demokritov, R. Kouba, R. Bozinoski, A. N. Slavin, K. Y. Guslienko, D. V. Berkov, N. L. Gorn, and et al., “Spin-wave excitations in finite rectangular elements of ni80fe20,” *Physical Review B* **72** (2005), 10.1103/physrevb.72.064427.
- ⁴⁰ Roman Verba, Mario Carpentieri, Giovanni Finocchio, Vasil Tiberkevich, and Andrei Slavin, “Excitation of propagating spin waves in ferromagnetic nanowires by microwave voltage-controlled magnetic anisotropy,” *Scientific Reports* **6** (2016), 10.1038/srep25018.
- ⁴¹ Roman Verba, Mario Carpentieri, Giovanni Finocchio, Vasil Tiberkevich, and Andrei Slavin, “Excitation of spin waves in an in-plane-magnetized ferromagnetic nanowire using voltage-controlled magnetic anisotropy,”

- Physical Review Applied **7** (2017), 10.1103/physrevapplied.7.064023.
- ⁴² S Klingler, A V Chumak, T Mewes, B Khodadadi, C Mewes, C Dubs, O Surzhenko, B Hillebrands, and A Conca, “Measurements of the exchange stiffness of yig films using broadband ferromagnetic resonance techniques,” *Journal of Physics D: Applied Physics* **48**, 015001 (2014).
- ⁴³ B. A. Auld, *Acoustic Fields and Waves in Solids* (Krieger Pub Co, 1990).
- ⁴⁴ M. Weiler, L. Dreher, C. Heeg, H. Huebl, R. Gross, M. S. Brandt, and S. T. B. Goennenwein, “Elastically driven ferromagnetic resonance in nickel thin films,” *Physical Review Letters* **106** (2011), 10.1103/physrevlett.106.117601.
- ⁴⁵ P. G. Gowtham, T. Moriyama, D. C. Ralph, and R. A. Buhrman, “Traveling surface spin-wave resonance spectroscopy using surface acoustic waves,” *Journal of Applied Physics* **118**, 233910 (2015).
- ⁴⁶ J. Janušonis, C. L. Chang, T. Jansma, A. Gatilova, V. S. Vlasov, A. M. Lomonosov, V. V. Temnov, and R. I. Tobey, “Ultrafast magnetoelastic probing of surface acoustic transients,” *Physical Review B* **94** (2016), 10.1103/physrevb.94.024415.
- ⁴⁷ C. L. Chang, A. M. Lomonosov, J. Janusonis, V. S. Vlasov, V. V. Temnov, and R. I. Tobey, “Parametric frequency mixing in a magnetoelastically driven linear ferromagnetic-resonance oscillator,” *Physical Review B* **95** (2017), 10.1103/physrevb.95.060409.
- ⁴⁸ Vasily V. Temnov, Christoph Klieber, Keith A. Nelson, Tim Thomay, Vanessa Knittel, Alfred Leitenstorfer, Denys Makarov, Manfred Albrecht, and Rudolf Bratschitsch, “Femtosecond nonlinear ultrasonics in gold probed with ultrashort surface plasmons,” *Nature Communications* **4** (2013), 10.1038/ncomms2480.
- ⁴⁹ Roman Verba, Vasil Tiberkevich, and Andrei Slavin, “Influence of interfacial dzyaloshinskii-moriya interaction on the parametric amplification of spin waves,” *Applied Physics Letters* **107**, 112402 (2015).
- ⁵⁰ P. Pirro, T. Brächer, A. V. Chumak, B. Lägel, C. Dubs, O. Surzhenko, P. Görnert, B. Leven, and B. Hillebrands, “Spin-wave excitation and propagation in microstructured waveguides of yttrium iron garnet/Pt bilayers,” *Applied Physics Letters* **104**, 012402 (2014).
- ⁵¹ Arne Vansteenkiste, Jonathan Leliaert, Mykola Dvornik, Mathias Helsen, Felipe Garcia-Sanchez, and Bartel Van Waeyenberge, “The design and verification of mumax3,” *AIP Advances* **4**, 107133 (2014).